Acta Crystallographica Section B
Structural Science
ISSN 0108-7681

Absence of halogen···halogen interactions in chlorotrimethylsilane polymorphs

Roman Gajda, Kamil Dziubek and Andrzej Katrusiak*

Faculty of Chemistry, Adam Mickiewicz University, Grunwaldzka 6, 60-780 Poznań, Poland

Correspondence e-mail: katran@amu.edu.pl

Received 1 September 2005
Accepted 16 November 2005

The structures of *in situ* pressure-frozen chlorotrimethylsilane crystals, $(CH_3)_3SiCl$, have been determined at 0.23, 0.30 and 0.58 GPa. The molecular arrangements in the low-temperature and high-pressure phases are two-dimensionally isostructural, but different in the third perpendicular direction. Consequently, a striking similarity exists between the unit-cell dimensions of these polymorphs. The absence of short Cl···Cl contacts, both in the low-temperature or pressure-frozen phases of $(CH_3)_3SiCl$, has been rationalized in terms of the favoured packing patterns and comparable energies of halogen···halogen interactions and other van der Waals forces.

1. Introduction

Halogen···halogen interactions were postulated to be significant cohesion forces in crystals, which are responsible for halogen-atom contacts which are commensurate to or closer than the sum of their van der Waals radii. These contacts were defined as 'donor–acceptor' interactions, 'secondary' interactions, 'charge-transfer' interactions, interactions between the highest occupied molecular orbitals and the lowest unoccupied molecular orbitals, or as 'incipient electrophilic and nucleophilic attack' (Rosenfield *et al.*, 1977; Guru Row & Parthasarathy, 1981; Ramasubbu *et al.*, 1986; Desiraju & Parthasarathy, 1989). Presently, halogen···halogen contacts are commonly considered, apart from the hydrogen bonds, as the main type of intermolecular interactions responsible for molecular aggregation in crystals (Metrangolo & Resnati, 2001; Bosch & Barnes, 2002; Zaman *et al.*, 2004). Indeed, short halogen···halogen contacts are observed in most molecular crystals built of halogenated compounds (Madhavi *et al.*, 2000; Saha *et al.*, 2005). Most recently we have studied the crystal structures and transformations of 1,2-dichloroethane (Bujak *et al.*, 2004) and 1,1,2,2-tetrachloroethane (Bujak & Katrusiak, 2004). Both these compounds form crystal phases with the ethylene moieties ordered and disordered and it was found that the transformations between these phases considerably modify the Cl···Cl contacts. Thus, it appeared that the internal conformational disorder in the molecules competes with the specific intermolecular Cl···Cl contacts. On the other hand, it can be argued that the densely packed molecules interact with the outermost atoms and that these interactions are bound to change when the molecules and structures transform. From this point of view, the Cl···Cl contacts can be regarded as a natural consequence of the atomic location in molecules and not caused by significant differences between the energies of the Cl···Cl and other van der Waals interactions.

This controversy can be illustrated by intermolecular contacts observed in the crystals of triphenylchloromethane,

compared with that of chloromethane. Triphenylchloromethane is known to form three polymorphs: one $P\bar{3}$-symmetric polymorph and two $P\bar{1}$-symmetric ones (Kahr & Carter, 1992; Gerdil & Dunand, 1975). In all these polymorphs short Cl···Cl contacts exist between the molecules. Each of the polymorphic structures has several independent Cl···Cl contacts, the shortest of which are of 3.209 (Dunand & Gerdil, 1982), 3.264 and 3.268 Å (Kahr & Carter, 1992), respectively. On the other hand, there are no similarly short Cl···Cl contacts in the chloromethane structure; the shortest intermolecular Cl···Cl contact is 4.01 Å and the next shortest is 4.14 Å (Burbank, 1953). Of five polymorphic structures of 2-chloro-2-methylpropane (Wenzel & Schneider, 1982; Wilmers *et al.*, 1984; Tamari *et al.*, 2000) the structural data are available for only one in the Cambridge Structural Database (Version 5.26 with updates to February 2005, 338 445 entries; Allen, 2002) and no short Cl···Cl contacts are present in that structure (Tamari *et al.*, 2000). Thus, the systematically short Cl···Cl contacts in triphenylchloromethane are contrasted with the absence of such contacts in chloromethane or 2-chloro-2-methylpropane. Therefore, it still remains uncertain if the existence of short contacts in some of the structures results from the intermolecular attraction between the halogen atoms or if it is a simple consequence of crystal packing.

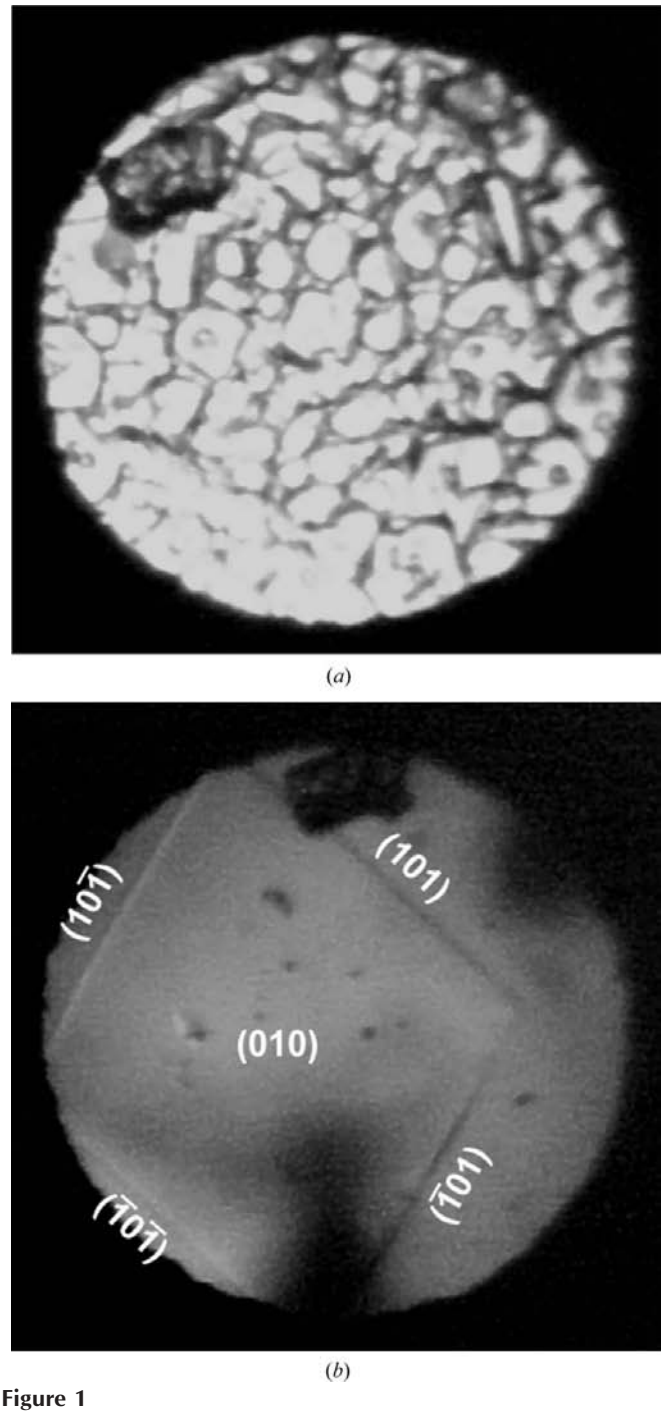

Figure 1
A view of the DAC high-pressure chamber with the pressure-frozen polycrystalline $(CH_3)_3SiCl$ at 0.23 GPa (*a*); (*b*) the single-crystal subsequently obtained under isochoric conditions at the initial stage of its growth. The ruby chip for pressure calibration has moved in the process of crystallization from the top-left (*a*) to the top (*b*) part of the pressure chamber. The Miller indices of the crystal in phase β have been given.

To investigate this controversy we have searched the literature for crystals of chlorinated compounds analogous to those described above, seeking the structures without short Cl···Cl contacts and without ionic or hydrogen-bond interactions. The crystal structure of chlorotrimethylsilane, $(CH_3)_3SiCl$, belongs to the group of structures without short Cl···Cl contacts – in fact it is isostructural with the known phase of 2-chloro-2-methylpropane. Compounds of small molecules such as $(CH_3)_3SiCl$, without strong cohesion forces, are liquids or gases under normal conditions. Therefore, $(CH_3)_3SiCl$ had to be frozen *in situ* at low temperature; there were no Cl···Cl contacts shorter than 4.9 Å in the structure determined (Buschmann *et al.*, 2000).

In this study we have attempted to force the $(CH_3)_3SiCl$ compound into a structure with shorter Cl···Cl contacts by applying high pressure, and to explain the reasons why the Cl···Cl contacts are not formed in the $(CH_3)_3SiCl$ or $(CH_3)_3CCl$ crystals obtained by low-temperature freezing. High pressures attainable in a diamond–anvil cell appeared to be ideal for this purpose, as the work performed on a molecular crystal at a fraction or a few GPa is comparable to the energy of intermolecular interactions in its structure. Thus, we hoped that by solving the high-pressure structures of $(CH_3)_3SiCl$ we would be able to contribute to the general understanding of molecular aggregation and intermolecular interactions in the crystals of halogenated compounds (Grineva & Zorky, 2000*a*,*b*, 2002; Metrangolo & Resnati, 2001; Bosch & Barnes, 2002; Zaman *et al.*, 2004).

2. Experimental

Chlorotrimethylsilane obtained from Aldrich (with purity higher than 99%) was used without further purification. It is a liquid at normal conditions and its m.p. is 215 K (Grasselli & Ritchey, 1975). A single crystal of $(CH_3)_3SiCl$ was grown *in situ* in a diamond–anvil cell (DAC) made in our departmental workshop of a modified Merril & Bassett (1974) design. The

Table 1
Selected experimental and crystal data for $(CH_3)_3SiCl$ in the high-pressure β phase (this work), compared with the low-temperature α phase (Buschmann *et al.*, 2000).

	Phase α	Phase β	Phase β	Phase β
Pressure	0.1 MPa	0.23 GPa	0.30 GPa	0.58 GPa
Temperature (K)	157	293	293	293
Crystal data				
Chemical formula	$(CH_3)_3SiCl$	$(CH_3)_3SiCl$	$(CH_3)_3SiCl$	$(CH_3)_3SiCl$
M_r	108.64	108.64	108.64	108.64
Cell setting	Monoclinic	Orthorhombic	Orthorhombic	Orthorhombic
space group	$P2_1/m$	$Pmn2_1$	$Pmn2_1$	$Pmn2_1$
a, b, c (Å)	6.2920 (10) 7.7350 (10) 6.745 (3)	7.785 (2) 6.43 (3) 6.254 (3)	7.768 (2) 6.42 (2) 6.233 (2)	7.668 (2) 6.34 (2) 6.159 (2)
β (°)	90.800 (10)	90	90	90
V (Å^3)	328.24 (16)	313.0 (15)	311.0 (11)	299.4 (11)
Z	2	2	2	2
D_x (Mg m^{-3})	1.099	1.153	1.160	1.205
Radiation type	0.71073	0.71073	0.71073	0.71073
No. of reflections for cell parameters	126	839	989	798
θ range (°)	8.0–17.3	4.18–27.40	4.19–22.45	4.24–24.90
μ (mm^{-1})	0.63	0.66	0.66	0.69
Crystal form, colour	Cylinder, colourless	Disc, colourless	Disc, colourless	Disc, colourless
Crystal size (mm)	0.8 × 0.3 × 0.3	0.46 × 0.46 × 0.18	0.44 × 0.44 × 0.18	0.42 × 0.42 × 0.18
Data collection				
Diffractometer	Siemens four-circle single-crystal X-ray diffractometer with an open χ circle of 100° and an integrated N_2 gas stream cooling device	Kuma KM4CCD κ geometry	Kuma KM4CCD κ geometry	Kuma KM4CCD κ geometry
Data collection method	ω–2θ scan; $\Delta\omega = 1.38° + 0.52° \times \tan\omega$	ω scans	ω scans	ω scans
Absorption correction	Analytical	Analytical	Analytical	Analytical
T_{min}	0.853	0.41	0.40	0.41
T_{max}	0.864	0.94	0.94	0.92
No. of measured, independent and observed reflections	1216, 971, 689	1793, 194, 170	1473, 164, 158	1697, 199, 193
Criterion for observed reflections	$I > 2\sigma(I)$	$I > 2\sigma(I)$	$I > 2\sigma(I)$	$I > 2\sigma(I)$
R_{int}	0.021	0.075	0.057	0.060
θ_{max} (°)	31.0	27.4	22.5	24.9
Range of h, k, l	$-3 \Rightarrow h \Rightarrow 8$ $-10 \Rightarrow k \Rightarrow 9$ $-9 \Rightarrow l \Rightarrow 9$	$-10 \Rightarrow h \Rightarrow 10$ $-1 \Rightarrow k \Rightarrow 1$ $-8 \Rightarrow l \Rightarrow 8$	$-8 \Rightarrow h \Rightarrow 8$ $-2 \Rightarrow k \Rightarrow 2$ $-6 \Rightarrow l \Rightarrow 6$	$-9 \Rightarrow h \Rightarrow 9$ $-2 \Rightarrow k \Rightarrow 2$ $-7 \Rightarrow l \Rightarrow 7$
Refinement				
Refinement on	F^2	F^2	F^2	F^2
$R[F^2 > 2\sigma(F^2)]$, $wR(F^2)$, S	0.037, 0.096, 1.12	0.032, 0.083, 1.01	0.032, 0.082, 1.22	0.039, 0.091, 1.27
No. of reflections	971	194	164	199
No. of parameters	47	29	32	29
H-atom treatment	Refined independently	Constrained refinement	Constrained refinement	Constrained refinement
Weighting scheme	$w = 1/[\sigma^2(F_o^2) + (0.0422P)^2 + 0.0947P]$, where $P = (F_o^2 + 2F_c^2)/3$	$w = 1/[\sigma^2(F_o^2) + (0.0568P)^2]$, where $P = (F_o^2 + 2F_c^2)/3$	$w = 1/[\sigma^2(F_o^2) + (0.0448P)^2 + 0.0802P]$, where $P = (F_o^2 + 2F_c^2)/3$	$w = 1/[\sigma^2(F_o^2) + (0.0395P)^2 + 0.1814P]$, where $P = (F_o^2 + 2F_c^2)/3$
$(\Delta/\sigma)_{max}$	<0.0001	<0.0001	0.223	<0.0001
$\Delta\rho_{max}$, $\Delta\rho_{min}$ (e Å^{-3})	0.45, −0.22	0.08, −0.10	0.11, −0.08	0.17, −0.19
Extinction method	None	*SHELXL*	*SHELXL*	*SHELXL*
Extinction coefficient	–	0.19 (3)	0.018 (17)	0.031 (17)
Flack parameter	–	0.6 (3)	0.2 (4)	0.0 (4)

gasket was made of 0.3 mm steel foil and the initial diameter of the hole was 0.5 mm. Immediately after filling the chamber with $(CH_3)_3SiCl$ the DAC screws were tightened until the sample froze in the polycrystalline form (see Fig. 1*a*). The DAC was then heated until all the crystallites but one were molten, after which the temperature was slowly lowered until this single crystal (Fig. 1*b*) grew to entirely fill the pressure chamber at room temperature. The pressure was calibrated to be 0.23 GPa with a BETSA PRL spectrometer by the ruby-fluorescence method with a precision of 0.05 GPa (Piermarini *et al.*, 1975). A single crystal of chlorotrimethylsilane was centered on a KUMA KM4 CCD diffractometer by the

gasket-shadow method (Budzianowski & Katrusiak, 2004). The X-ray reflections intensities were collected in the ω-scan mode (Budzianowski & Katrusiak, 2004). The Mo $K\alpha$ radiation was graphite-monochromated. The *CrysAlis* programs (Oxford Diffraction, 2003) were used for data collection, unit-cell refinement and initial data reduction. The data were corrected for DAC absorption, gasket shadowing and absorption of the sample itself (Katrusiak, 2003, 2004*a*); the unit-cell dimensions were corrected for the reflections shifts due to the gasket shadowing (Katrusiak, 2004*b*). The structure was solved by direct methods using the program *SHELXS*97 and refined using *SHELXL*97 (Sheldrick, 1997). Subsequently, the positions of the C, Cl and Si atoms were refined with anisotropic displacement parameters by *SHELXL*97. The H atoms have been located from the molecular geometry (C—H 0.97 Å, U_{iso} is equal to 1.2 of the U_{eq} value of their carriers); in the final cycles of the refinement the rigid idealized methyl group $C(2)H_3$ was allowed to rotate about the C—Si bond, while for the $C(1)H_3$ methyl two possible orientations of the idealized H atoms allowed by the symmetry were compared. After determining the structure at 0.23 GPa, the same procedure was repeated to obtain the single crystal data at 0.3 and 0.58 GPa. The structural drawings were prepared using the program *XP* (Sheldrick, 1998). The crystallographic data are given in Table 1.[1]

3. Discussion

The crystal data, compiled in Table 1, show that the low-temperature (Buschmann *et al.*, 2000) and high-pressure structures have different symmetries of the monoclinic space group $P2_1/m$ and the orthorhombic space group $Pmn2_1$, respectively. The temperature-frozen structure has been labelled phase α and the new pressure-frozen structure phase β. The α phase of chlorotrimethylsilane is isostructural to phase IV of 2-chloro-2-methylpropane and also to phase II of $(CH_3)_3CCN$ (Tamari *et al.*, 2000). None of the presently known phases of these compounds are isostructural with new phase β of $(CH_3)_3SiCl$. The low-temperature and high-pressure unit-cell parameters have been compared in Table 1 and in Fig. 2. A striking feature of phases α and β is that despite different symmetries their unit-cell dimensions are very similar. It is apparent that a_α corresponds to c_β, b_α to a_β and c_α to b_β (the subscripts denote the unit-cell dimensions of polymorphs α and β). Furthermore, the c_β parameter at 0.23 GPa is only 0.038 Å shorter than a_α at 0.1 MPa and 157 K, and a_β is only 0.05 Å longer than b_α. In both phases the number of molecules in the unit cell (Z) and the molecular site symmetries are the same. In both phases α and β the $(CH_3)_3SiCl$ molecule occupies a special position on the mirror plane. The Cl1, Si1, C1 and H11 atoms lie on that plane (Fig. 3).

It is apparent that the similar unit-cell dimensions are not accidental, but originate from the molecular dimensions and interactions. As can be seen from Fig. 4 the molecular arrangements are nearly identical when structures α and β are projected down $\mathbf{b}_\alpha$ and $\mathbf{c}_\beta$, respectively. The main difference between structures α and β is that every second row of molecules, as viewed in Fig. 5, is rotated by 180° about the direction perpendicular to the drawing. Owing to the specific symmetry of the molecule, the same effect can be achieved by rotating each molecule in every second row in Fig. 5 by 60° around the Si—Cl bond.

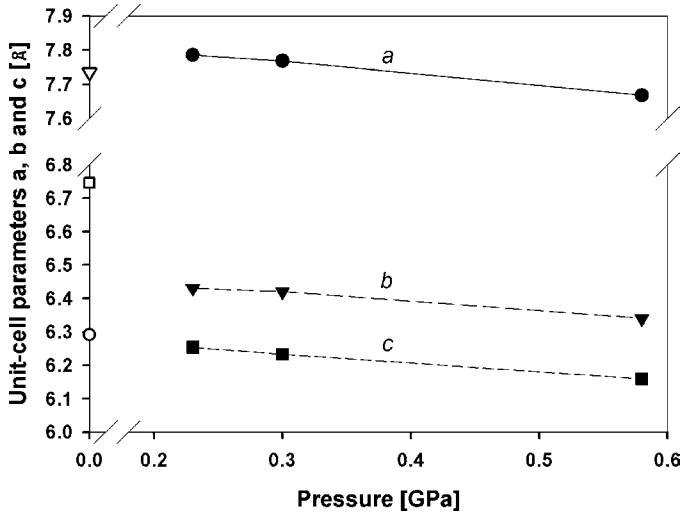

Figure 2
The unit-cell dimensions a, b and c of phase α of $(CH_3)_3SiCl$ at 0.1 MPa (empty circle, empty triangle and empty square, respectively), and the pressure dependence of parameters a, b and c of the β phase (filled symbols).

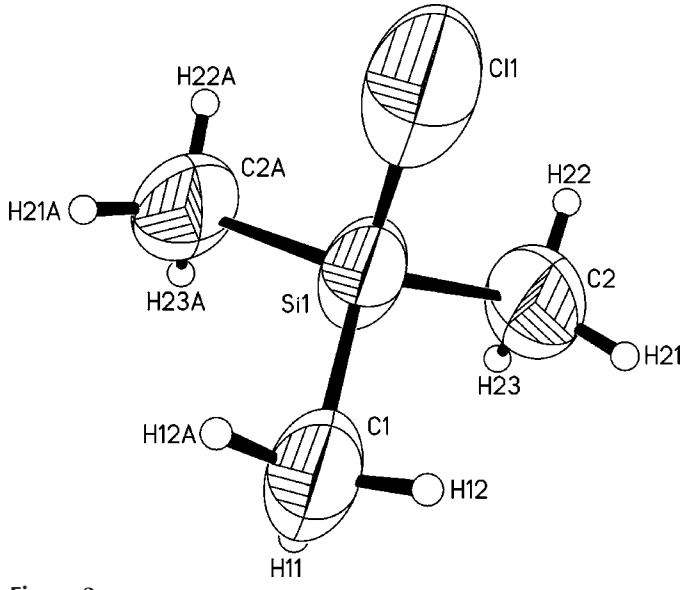

Figure 3
A molecule of chlorotrimethylsilane as determined in the crystal structure at 0.30 GPa. The displacement ellipsoids have been drawn at the 50% probability level. The letter '*A*' has been added to the atomic label to denote the atoms generated by the mirror plane, passing through the atoms C1, Si1 and Cl1.

[1] Supplementary data for this paper are available from the IUCr electronic archives (Reference: AV5043). Services for accessing these data are described at the back of the journal.

Analogous to the nomenclature of one-, two- and three-dimensional isostructurality introduced by Fábián & Kálmán (2004), phases α and β of $(CH_3)_3SiCl$ can be described as one-dimensional polymorphs. According to Fábián & Kálmán (2004), and as can be seen from Fig. 4, phases α and β are isostructural in two dimensions, but different in the third perpendicular direction, as viewed clearly in Fig. 6. It can be observed that the unit cell in the high-pressure β phase becomes more elongated along one direction (a_β) and narrower along two others (b_β and c_β), compared with the unit cell of phase α (Fig. 2). As a consequence, the distances between the centers of the molecules (the Si atoms) become longer in the β phase (Fig. 7), despite the smaller molecular volume. Also, the Cl···Cl and Cl···Si distances become longer in the β phase. The considerable shortening is observed between Cl···C2, and smaller shortening between Cl···C1.

The unit-cell parameters of phase β compress at a similar rate. Parameter b has large standard deviations (Table 1) because reflections with large Miller indices k could not be

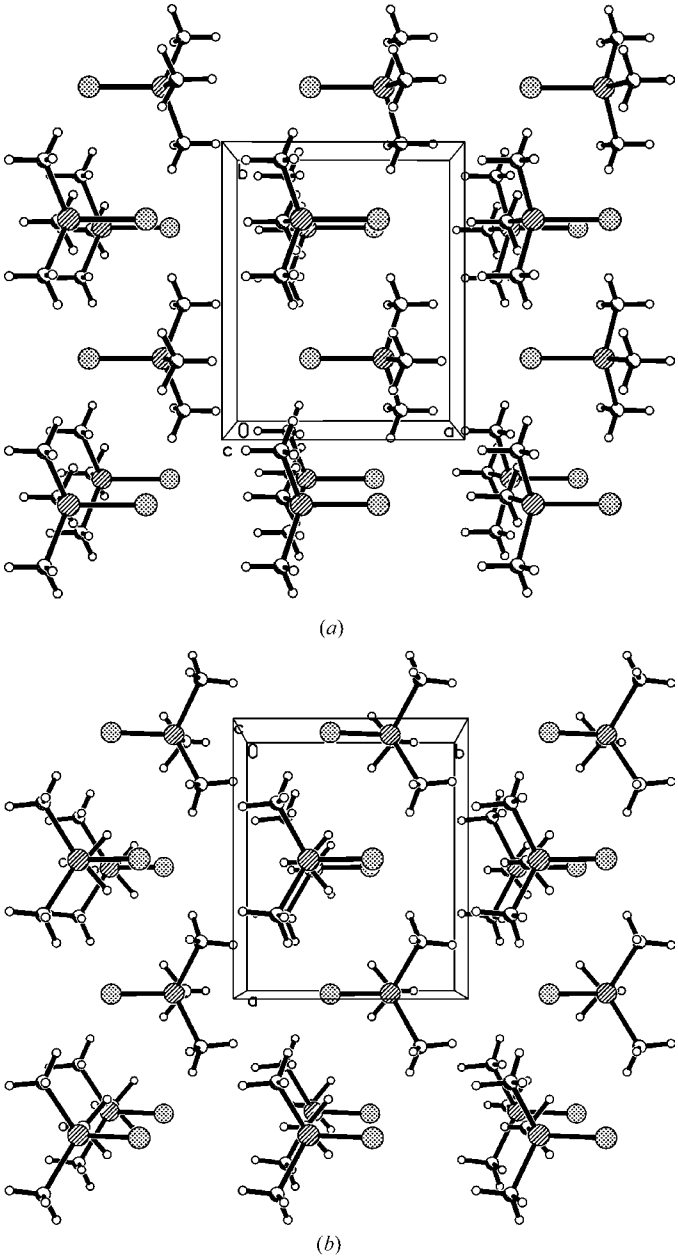

Figure 4
Autostereograms (Katrusiak, 2001) of the $(CH_3)_3SiCl$ structures in: (*a*) the low-temperature α phase; (*b*) the high-pressure β phase.

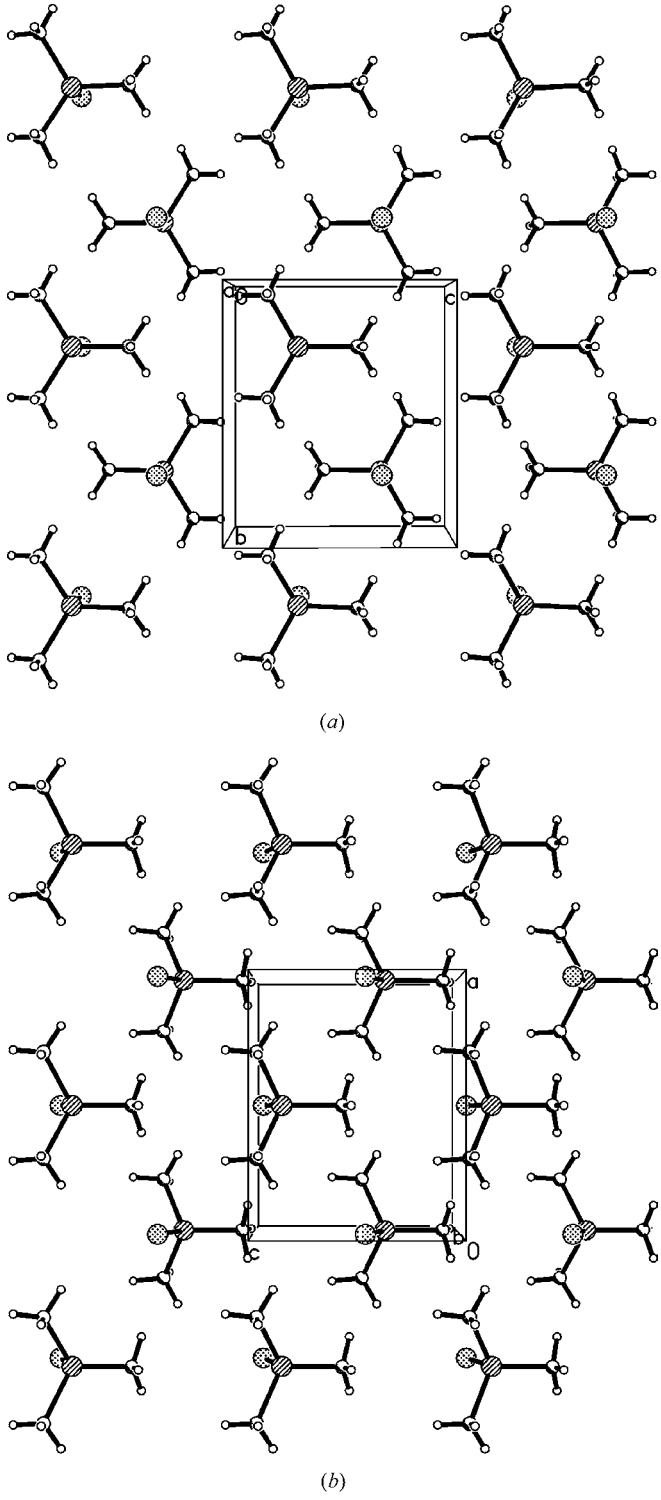

Figure 5
Autostereographic projection (Katrusiak, 2001) of the $(CH_3)_3SiCl$ structures: (*a*) polymorph α viewed down **a**; (*b*) polymorph β viewed down **b**.

Table 2
Selected molecular dimensions (Å, °) of $(CH_3)_3SiCl$ in phase α at 0.1 MPa and 157 K (Buschmann *et al.*, 2000), and in phase β (this work).

Phase P/T	α 0.1 MPa and 157 K	β 0.23 GPa and 296 K	β 0.30 GPa and 296 K	β 0.58 GPa and 296 K
Cl1—Si1	2.0863 (9)	2.010 (15)	2.02 (2)	1.988 (14)
Si1—C1	1.845 (3)	1.882 (9)	1.808 (10)	1.825 (9)
Si1—C2	1.843 (3)	1.964 (19)	1.869 (15)	1.878 (12)
C1—Si1—Cl1	106.92 (12)	115.4 (10)	109.2 (10)	109.4 (10)
C2—Si1—Cl1	106.57 (9)	114.3 (10)	106.8 (7)	106.7 (7)
C1—Si1—C2	111.87 (11)	105.9 (7)	111.3 (5)	111.3 (5)
C2—Si1—C2^{i}	112.6 (2)	99.3 (16)	111.4 (14)	111.2 (12)

Symmetry codes: (i) $x, \frac{1}{2}-y, z$ in phase α; $-x, y, z$ in phase β.

measured due to the specific orientation of the crystals in the DAC (*cf.* Fig. 1). The molecular volume V_m of $(CH_3)_3SiCl$ in the liquid phase, equal to 212.2 Å^3 at 293 K, reduces to 164.1 Å^3 as the result of isobaric temperature contraction of the liquid, volume contraction on freezing and solid-phase α contraction to 157 K. The isothermal compression of the liquid, the volume change at pressure freezing and the compression of solid $(CH_3)_3SiCl$ in phase β lead to the molecular volumes 156.6, 155.5 and 149.7 Å^3 at 0.23, 0.30 and 0.58 GPa, respectively. Unfortunately, no experimental measurements of the compression of liquid $(CH_3)_3SiCl$ could be found and the volume of fusion could not be determined from our measurements.

The Si—Cl bond lengths in phase β (Table 2) are slightly shorter than in phase α at ambient pressure; only the least precise dimensions determined at 0.3 GPa agree within error. The C—Si bond length in organosilicon compounds depends on its chemical environment. The longest bonds occur in crowded molecules, whereas electronegative ligands at silicon, like chlorine, shorten the C—Si bond by removing electron density from the Si atom (Campanelli *et al.*, 2000). However, the effects of pressure and molecular packing on the C—Si bond length cannot be reliably assessed because of these structural determinations.

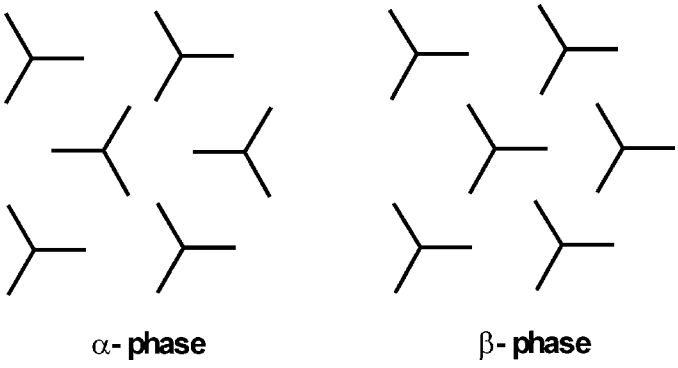

Figure 6
Schematic representation of (*a*) phase α and (*b*) phase β. The molecules are projected along the Si—Cl bond in the orientations analogous to those shown in Fig. 5.

The shortening of the Cl···C contacts can be due to methyl rotations being efficiently hindered by pressure. The elongation of the Cl···Cl distances in phase β and the shortening of Cl···C distances may be caused by the electrostatic contribution to the interactions between these atoms. The absence of short Cl···Cl contacts in phases α and β is consistent in certain aspects with the chlorophobic effect postulated for chlorinated aromatic compounds by Grineva & Zorky (1998, 2000*a*).

It is well known that the process of crystallization imposes restrictions on the conformation and symmetry of molecules, leading to their dense packing in the crystal (Kitajgorodski, 1976). The dense packing, in other words, can be described as the molecular arrangement maximizing the number of intermolecular contacts. Neither of the molecular packing modes in phases α and β of $(CH_3)_3SiCl$ involve short Cl···Cl contacts. The molecular arrangements in crystal structures usually satisfy the dense-packing condition (Kitajgorodski, 1976), which does not necessarily coincide with the energy hierarchy of specific types of intermolecular interactions of atoms.

The absence of short inter-halogen contacts in $(CH_3)_3SiCl$ has been related to the shortest intermolecular Cl···Cl distances determined with high precision ($R \leq 0.075$) in fully ordered structures of chlorinated hydrocarbons, optionally containing silicon, which were retrieved from the Cambridge Structural Database (Version 5.26 with updates to February 2005, 338 445 entries; Allen, 2002). Only homomolecular crystals (*i.e.* consisting of one type of molecule) have been considered. Of several structures determined at different

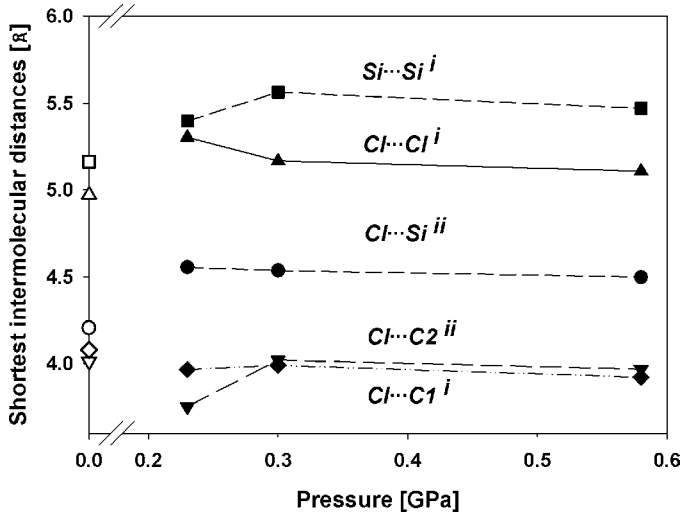

Figure 7
The closest intermolecular distances in phase α (empty symbols), phase β (full symbols) and their pressure dependence. The symmetry transformations used to generate equivalent atoms in phase β are: (i) $\frac{1}{2}-x, 1-y, -\frac{1}{2}+z$; (ii) $x, 1+y, z$.

temperatures only the one measured at the temperature closest to 295 K was retained; in the case of the same experimental conditions, the most accurate structure was selected (with the lowest *R* factor). The database has been searched using the nonbonded-contacts-query procedure to retrieve the intermolecular Cl···Cl distances. Although similar surveys have already been reported (Rowland & Taylor, 1996), they dealt with the total number of contacts up to a pre-set distance cut-off equal to the sum of van der Waals radii, plus a fixed tolerance. For the purpose of our study we inspected the shortest contacts from each structure only. The histogram of Cl···Cl distances obtained in this manner has been plotted for 0.1 Å intervals in Fig. 8.

As expected, the distribution is skewed: steep at the short-contacts side consistent with a strong repulsion and with an elongated tail on the long-contact side (right), which could be interpreted as evidence of the energetic preference for close packing rather than Cl···Cl interactions. The behaviour of silylated derivatives is analogous, but a paucity of observations hampers the critical assessment of this tendency. Indeed it has already been indicated by Price *et al.* (1994) that the energetic contribution of the halogen···halogen interactions for the aggregation of molecules is not substantial, which is particularly manifested in lightly chlorinated compounds (with a low number of Cl atoms compared with the number of H atoms). To illustrate this phenomenon a scatter plot of the shortest contacts in the function of the H/Cl ratio has been shown in Fig. 9.

An immediate conclusion is that the preponderance of short contacts is reduced with decreasing chlorine content, although even for the lightly chlorinated hydrocarbons short Cl···Cl distances can also appear (*e.g.* triphenylchloromethane). It is apparent that steric hindrances and molecular packing are significant factors, which may compete with intermolecular interactions of individual atoms. It was demonstrated that for the crystals of monoalcohols, the molecules of which usually aggregate due to OH---O hydrogen-bond attraction, in certain cases the OH---O hydrogen bonds could not be formed due to steric hindrances and crystal packing (Brock & Duncan, 1994; Taylor & Macrae, 2001). Thus, the existence of such structures, despite the fact that the OH---O hydrogen bonds are undoubtedly attractive, may support the conclusion that an analogous situation could exist for the interactions and the formation of intermolecular Cl···Cl contacts in the chlorinated compounds. In the case of weakly chlorinated compounds the rate of the absence of Cl···Cl contacts is incomparably higher than in monoalcohols: 65% for monochlorinated compounds and 27% for dichlorinated ones (Grineva & Zorky, 2000*b*). This testifies that the contribution of the Cl···Cl contacts to the crystal cohesion is small.

4. Conclusions

The structure of the new high-pressure β phase of $(CH_3)_3SiCl$ is two-dimensionally isostructural and one-dimensionally polymorphic to the α phase. The unit-cell dimensions of phases α and β differ by up to 6% and only a small shortening in the intermolecular Cl···C distances by 6.5% and a lengthening of the Cl···Cl distances by 6.7% have been observed. This pressure dependence, as well as the absence of the short Cl···Cl contacts commensurate with the sums of the van der Waals radii, in both phases α and β may be a consequence of the Cl···Cl attraction being comparable to, or weaker than, other van der Waals interactions in these structures. The temperature and pressure dependence of the $(CH_3)_3SiCl$ crystal is considerably different than that of the analogous $(CH_3)_3CCl$ crystal, which exhibits five known crystal phases in the 100–250 K and 0.1–300 MPa ranges. Whereas these two compounds are isostructural at low temperatures [$(CH_3)_3SiCl$ in phase α and $(CH_3)_3CCl$ in phase IV], $(CH_3)_3CCl$ also forms a plastic phase above 220 K and a partly disordered tetragonal phase between 217 and 183 K, neither of which were observed for $(CH_3)_3SiCl$. At present only two phases, α and β, of

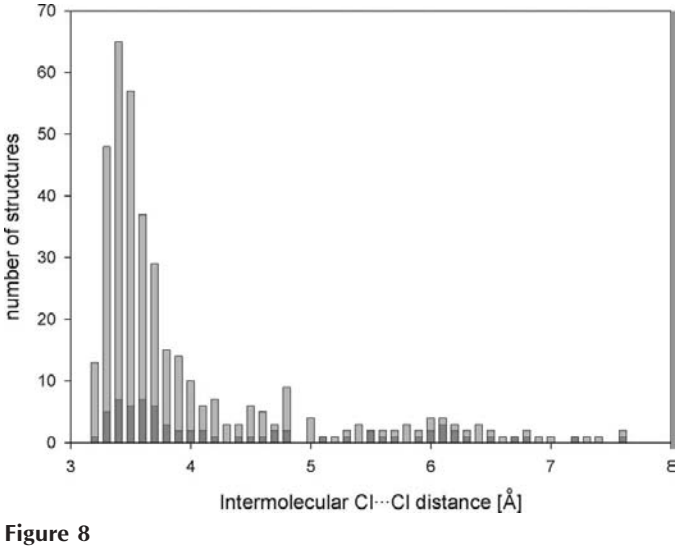

Figure 8
Histogram of Cl···Cl distance distribution in 312 structures of chlorinated hydrocarbons (gray bars) and 69 structures of chlorinated silahydrocarbons (dark gray bars).

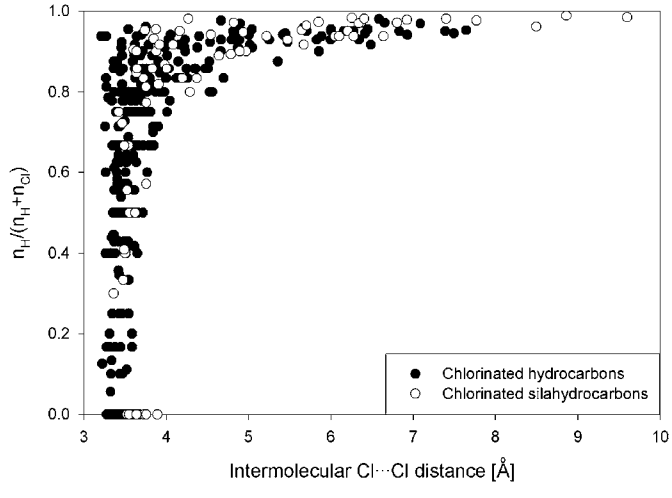

Figure 9
The scatterplot of the shortest intermolecular Cl···Cl contacts as a function of the ratio of the numbers of H and Cl atoms.

$(CH_3)_3SiCl$ are known. On the other hand, the new β phase of $(CH_3)_3SiCl$ described in this paper may have some common features with the high-pressure phase of $(CH_3)_3CCl$ described by Wilmers *et al.* (1984). The structural and thermodynamic relations between these analogous compounds are currently under study.

This study was supported by the Polish Ministry of Scientific Research and Information Technology, Grant No. 3 T09A18127. The authors would like to thank Mr Armand Budzianowski for his help with data reduction.

References

Allen, F. H. (2002). *Acta Cryst.* B**58**, 380–388.
Bosch, E. & Barnes, C. L. (2002). *Cryst. Growth Des.* **4**, 299–302.
Brock, C. P. & Duncan, L. L. (1994). *Chem. Mater.* **6**, 1307–1312.
Budzianowski, A. & Katrusiak, A. (2004). *High-Pressure Crystallography*, edited by A. Katrusiak & P. F. McMillan, pp. 101–111. Dordrecht: Kluwer Academic Publishers.
Bujak, M., Budzianowski, A. & Katrusiak, A. (2004). *Z. Kristallogr.* **219**, 573–579.
Bujak, M. & Katrusiak, A. (2004). *Z. Kristallogr.* **219**, 669–674.
Burbank, R. D. (1953). *J. Am. Chem. Soc.* **75**, 1211–1214.
Buschmann, J., Lentz, D., Luger, P. & Röttger, M. (2000). *Acta Cryst.* C**56**, 121–122.
Campanelli, A. R., Ramondo, F., Domenicano, A. & Hargittai, I. (2000). *Struct. Chem.* **11**, 155–160.
Desiraju, G. R. & Parthasarathy, R. (1989). *J. Am. Chem. Soc.* **111**, 8725–8726.
Dunand, A. & Gerdil, R. (1982). *Acta Cryst.* B**38**, 570–575.
Fábián, L. & Kálmán, A. (2004). *Acta Cryst.* B**60**, 547–558.
Gerdil, R. & Dunand, A. (1975). *Acta Cryst.* B**31**, 936–937.
Grasselli, J. G. & Ritchey, W. M. (1975). Editors. *CRC Atlas of Spectral Data and Physical Constants for Organic Compounds*, 2nd Ed. New York: CRC Press Inc.
Grineva, O. V. & Zorky, P. M. (1998). *Zh. Fiz. Khim.* **72**, 714–720 (in Russian).
Grineva, O. V. & Zorky, P. M. (2000*a*). *Kristallografiya*, **45**, 692–698 (in Russian).
Grineva, O. V. & Zorky, P. M. (2000*b*). *Zh. Fiz. Khim.* **74**, 1937–1943 (in Russian).
Grineva, O. V. & Zorky, P. M. (2002). *Zh. Strukt. Khim.* **43**, 1073–1083 (in Russian).
Guru Row, T. N. & Parthasarathy, R. (1981). *J. Am. Chem. Soc.* **103**, 477–479.
Kahr, B. & Carter, R. L. (1992). *Mol. Cryst. Liq. Cryst.* **219**, 79–100.
Katrusiak, A. (2001). *Mol. Graph. Model.* **19**, 363–367.
Katrusiak, A. (2003). *REDSHAD*. Adam Mickiewicz University, Poznań.
Katrusiak, A. (2004*a*). *Z. Kristallogr.* **219**, 461–476.
Katrusiak, A. (2004*b*). *REDSHUB*. Adam Mickiewicz University, Poznań.
Kitajgorodski, A. I. (1976). *Kryształy molekularne.* Warsaw: PWN (in Polish).
Madhavi, N. N. L., Desiraju, G. R., Bilton, C., Howard, J. A. K. & Allen, F. H. (2000). *Acta Cryst.* B**56**, 1063–1070.
Merril, L. & Bassett, W. A. (1974). *Rev. Sci. Instrum.* **45**, 290–294.
Metrangolo, P. & Resnati G. (2001). *Chem. Eur. J.* **7**, 2511–2519.
Oxford Diffraction, (2003). *CrysAlis CCD* and *CrysAlis RED*, GUI versions. Oxford Diffraction, Poland.
Piermarini, G. J., Block, S., Barnett, J. D. & Forman, N. A. (1975). *J. Appl. Phys.* **46**, 2774–2780.
Price, S. L., Stone, A. J., Lucas, J., Rowland, R. S. & Thornley, A. E. (1994). *J. Am. Chem. Soc.* **116**, 4910–4918.
Ramasubbu, N., Parthasarathy, R. & Murray-Rust, P. (1986). *J. Am. Chem. Soc.* **108**, 4308–4314.
Rosenfield, R. E., Parthasarathy, R. & Dunitz, J. D. (1977). *J. Am. Chem. Soc.* **99**, 4860–4862.
Rowland, R. S. & Taylor, R. (1996). *J. Phys. Chem.* **100**, 7384–7391.
Saha, B. K., Jetti, R. K. R. & Reddy, L. S. (2005). *Cryst. Growth. Des.* **5**, 887–899.
Sheldrick, G. M. (1998). *SHELXTL*, Version 5.1. Siemens Analytical X-ray Instrument Inc., Madison, Winsconsin, USA.
Sheldrick, G. M. (1997). *SHELXS*97 and *SHELXL*97. University of Göttingen, Germany.
Tamari, J. L., Lopez, D. O., Alcobe, X., Barrio, M., Salud, J. & Pardo, L. C. (2000). *Chem. Mater.* **12**, 555–563.
Taylor, R. & Macrae, C. F. (2001). *Acta Cryst.* B**57**, 815–827.
Wenzel, U. & Schneider, G. M. (1982). *Mol. Cryst. Liq. Cryst. (Lett.)* **72**, 255–261.
Wilmers, J., Briese, M. & Würflinger, A. (1984). *Mol. Cryst. Liq. Cryst.* **107**, 293–302.
Zaman, B., Udachin, K. A. & Ripmeester, J. A. (2004). *Cryst. Growth Des.* **3**, 585–589.